Thermochimica Acta, 69 (1983) 341–348
Elsevier Science Publishers B.V., Amsterdam – Printed in The Netherlands

THE INFLUENCE OF PARTICLE SHAPE ON THE NON-ISOTHERMAL KINETICS OF PRECIPITATE DISSOLUTION

ARI VARSCHAVSKY and EDUARDO DONOSO

Universidad de Chile, Facultad de Ciencias Físicas y Matemáticas, Instituto de Investigaciones y Ensayes de Materiales (IDIEM), Casilla No. 1420, Santiago (Chile)

(Received 14 April 1983)

ABSTRACT

Based on the theory of precipitate dissolution kinetics proposed by Whelan, two expressions suitable for use under non-isothermal conditions were derived. The first one arises from the transient part of the diffusion field and it is found to be identical to that known as the three-dimensional diffusion kinetic law, being instead the reflection of a one-dimensional diffusion process. The second relationship which arises essentially from the steady-state part of the diffusion field, better describes a three-dimensional diffusion situation, being the corresponding kinetic model function in the integrated form: $f(y) = 1-(1-y)^{2/3}$. The first solution was successfully applied for describing the dissolution behaviour of disc-shaped G.P. zones in 2219 aluminium under non-isothermal conditions, while the second was valid for description, under the same conditions, of the dissolution kinetics of spherical ordered domains in two αCu–Al alloys.

INTRODUCTION

Rate equations used for homogeneous reactions [1] (gaseous phases or liquid solutions) where collisions are involved between freely moving particles, have often been employed to describe solid-state reactions under isothermal and non-isothermal conditions. In particular, a first-order kinetic law was used by several authors for describing the dissolution behaviour of second phase precipitates [2,3] under non-isothermal conditions. Such a relationship, therefore, has little physical justification and the required value of the activation energy cannot be simply related to a physical process in a specific system.

Diffusion limited dissolution kinetic models have been developed by Aaron [4] and Whelan [5] under conditions where concentration gradients were absent from the two phases prior to the solution treatment. The first model assumes one-dimensional flow, linear gradients during solution, and semi-infinite concentration–distance profiles, while the second provides an error function profile rather than a linear gradient, and also considers a spherical flow solution model. Tanzilli and Heckel [6,7] have shown the

0040-6031/83/$03.00

applicability of numerical methods, eliminating the necessity for simplifying assumptions. However, these procedures are not very suitable for use in kinetic determinations under non-isothermal conditions, since the task of deriving appropriate solutions is cumbersome.

In the present study, a method of analysis for obtaining kinetic equations based on physical models taking account of the decrease in the precipitate half thickness or radius under diffusion limited conditions is developed. The results are applied to the description of the non-isothermal kinetics of dissolution of G.P. zones in aluminium alloy 2219 and to the dissolution of disperse ordered particles in αCu-10 and 15 at.% Al alloys.

THEORETICAL CONSIDERATIONS

From the relationships giving the concentration profile and the flux of the solute at the interface of a dissolving spherical precipitate of radius r at time t [5,8], the following differential equation is obtained for the instantaneous radius of the precipitate

$$\frac{dr}{dt} = -\frac{kD}{2r} - \frac{k}{2}\sqrt{\frac{D}{\pi t}} \tag{1}$$

where D is the volume diffusion coefficient in the matrix; $k = 2(c_I - c_M)/(c_p - c_I)$, c_I is the concentration in the matrix at the precipitate–matrix interface, c_M is the solute concentration in the matrix and c_p is the composition of the precipitate. The exact solution of eqn. (1) is rather complicated, but it appears reasonable to obtain approximate solutions, peculiar to specific situations, which makes them useful for their relative simplicity.

For a planar interface, the term r^{-1}, which arises from the steady-state part of the diffusion field [5], does not contribute to the rate of dissolution, hence, eqn. (1) integrates under isothermal conditions to

$$r = r_0 - \frac{k}{\sqrt{\pi}}\sqrt{Dt} \tag{2}$$

where r_0 is the initial half-thickness of the precipitate. Equation (2) is identical to the Aaron model for precipitate dissolution. If the term $t^{-1/2}$, which arises from the transient part of the diffusion field [5], is neglected (e.g. for long times), the solution of eqn. (1) for the same conditions yields

$$r^2 = r_0^2 - kDt \tag{3}$$

where r_0 is the precipitate radius in this case. This is the equation given by Thomas and Whelan [9].

The next step is to transform eqns. (2) and (3) into suitable expressions for kinetic analysis in terms of the reacted fraction, y, which is related to the

volume fraction, V_f, of the precipitates by

$$y = 1 - V_f = 1 - \left(\frac{r}{r_0}\right)^3 \tag{4}$$

From eqns. (2) and (4) we get

$$\left[1 - (1-y)^{1/3}\right]^2 = \frac{K_1 t}{r_0^2} \tag{5}$$

in which K_1/r_0^2 is the equivalent rate constant and $K_1 = k^2 D/\pi$. If we assume that the temperature dependence of the reaction-rate constant follows an Arrhenius equation, as may be expected from its major dependence on the diffusion coefficient, eqn. (5) becomes

$$\left[1 - (1-y)^{1/3}\right]^2 = \frac{K_{01}}{r_0^2}\left[\exp\left(-\frac{E}{RT}\right)\right]t \tag{6}$$

where E is close to the activation energy for chemical interdiffusion, K_{01} is a constant and R is the universal gas constant. Equation (5) or (6) represents a deceleratory y vs. t curve, inadequately termed a three-dimensional diffusion law according to a broad classification of solid-state rate expressions [10]. This law was originally developed to describe the kinetics of reactions in powders [11] and it is suitable essentially for one-dimensional diffusion situations.

Also, from eqns. (3) and (4), an unclassified rate equation according to ref. 10 can be derived, which describes essentially three-dimensional diffusion controlled situations, i.e.

$$1 - (1-y)^{2/3} = \frac{K_2}{r_0^2} t \tag{7}$$

where $K_2 = kD$ in this case. By the same arguments as those given earlier

$$1 - (1-y)^{2/3} = \frac{K_{02}}{r_0^2}\left[\exp\left(-\frac{E}{RT}\right)\right]t \tag{8}$$

where K_{02} is a constant. Equations (6) and (8) are the basis for describing non-isothermal experimental conditions.

Following the usual approach to non-isothermal kinetics in thermal analysis [10,12], the reacted fraction solved from eqn. (6) becomes

$$y = 1 - \left\{1 - \left[\frac{EK_{01}}{\alpha R r_0^2} p(x)\right]^{1/2}\right\}^3 \tag{9}$$

when a linear heating rate $\alpha (= \mathrm{d}T/\mathrm{d}t)$ is employed. Similarly, under these conditions y can be written from eqn. (8) as

$$y = 1 - \left[1 - \frac{EK_{02}}{\alpha R r_0^2} p(x)\right]^{3/2} \tag{10}$$

where $x = E/RT$ and

$$p(x) = \int_0^x \frac{\exp(-x)}{x^2} dx \simeq (x+2)^{-1} x^{-1} \exp(-x) \tag{11}$$

if the three-dimensional Schlomilch expression [12] is used. Both expressions [(9) and (10)] give sigmoidal y vs. T curves.

RESULTS AND DISCUSSION

The foregoing analysis is used to describe the non-isothermal dissolution kinetics of two types of particles: G.P. zones in 2219 Al and disperse order in two α-CuAl alloys.

In order to identify the kinetic equation governing the non-isothermal dissolution kinetics of a particular precipitate, it is convenient to integrate the reaction peak in a DTA (ΔT vs. T) or DSC (ΔC_p vs. T) curve in a stepwise manner. The fraction reacted at a given temperature, y, is defined as the ratio of the area of the peak up to that temperature, A_T, to the total area of the peak, A_F. With this procedure, the experimental thermogram can be converted into a y vs. T curve which always shows a sigmoidal shape, allowing direct comparison with an appropriate selected relationship [e.g. eqns. (9) or (10)].

G.P. zone dissolution in 2219 aluminium alloy

The dissolution kinetics of G.P. zones in this alloy were analysed by employing the experimental y vs. T curves for two specific microstructural conditions reported by Papazian [13] which resulted from the following aging conditions: (a) 2.2 days at 130°C and (b) 10 days at 75°C. After the first treatment, the sample contained G.P. zones of 5.0 nm radius. In this study, eqn. (9) was fitted to the experimental y vs. T curve obtained from condition (a) using $r_0 = 5$ nm and $E = 126$ kJ mole^{-1}, which is the activation energy for chemical interdiffusion in the Al–Cu system [14]. This fit gave a value of $K_{01} = 5.7 \times 10^{15}$ nm^2 s^{-1}. The experimental y vs. T curve (solid line) and the calculated curve (broken line) are shown in Fig. 1(a). Using these values for K_{01} and E, eqn. (9) was again fitted to the experimental y vs. T curve corresponding to treatment (b) [Fig. 1(b), solid line] by adjusting the zone radius. This procedure resulted in a calculated curve [Fig. 1(b), broken line] which predicts $r_0 = 1.5$ nm. The G.P. zone radius of a sample subjected to treatment (b) was measured using TEM, and found to be 1.95 ± 0.2 nm [13].

If an identical procedure is employed by fitting eqn. (10) to the experimental y vs. T curve corresponding to the 5 nm G.P. zone radius, a value of $K_{02} = 3.83 \times 10^{13}$ nm^2 s^{-1} was obtained. The best fits which can be achieved

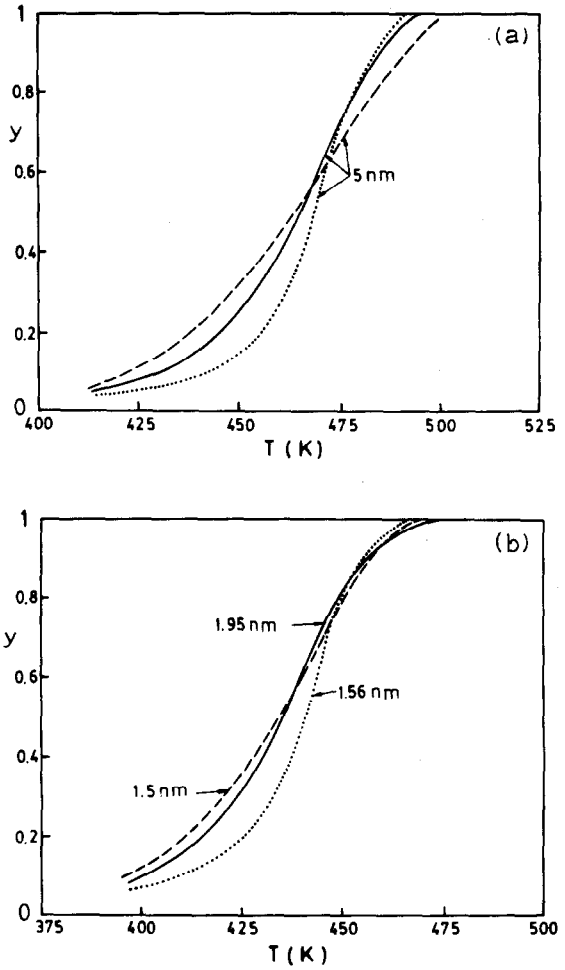

Fig. 1. (a) Experimental and calculated y vs. T curves for G.P. zone dissolution in 2219 Al alloys for aging treatment (a). ———, Experimental curve; - - - - - -, calculated from eqn. (9); · · · · · ·, calculated from eqn. (10). Particle radius taken to be 5 nm. (b) Experimental and calculated y vs. T curves for G.P. zone dissolution in 2219 Al alloys for aging treatment (b). ———, Experimental curve; - - - - - -, calculated from eqn. (9); · · · · · ·, calculated from eqn. (10). Zone radius as indicated.

for both aging treatments are shown in Fig. 1(a) and (b) (dotted lines). In this case, $r_0 = 1.56$ nm resulted from treatment (b).

Although both kinetic model functions give similar values for zone radii, the calculated curves from eqn. (9) fit much better to the shape of the experimental y vs. T curves. This result can be attributed to the fact that the actual dissolution behaviour of disc-shaped zones differs from predictions based on an assumed spherical geometry, where three-dimensional diffusion takes place. In this way the dissolution kinetics may essentially be described by a model suitable for a planar interface and one-dimensional diffusion, as

expected. It should also be noted that the chosen value for the activation energy (126 kJ mole^{-1}), equal to the activation energy for chemical interdiffusion in the Al–Cu system [14], provides an additional physical basis for the satisfactory results predicted by eqn. (9).

Disperse order dissolution in Cu-10 at.% and 15 at.% Al alloys

Following a similar treatment as in the previous section, the dissolution kinetics of the ordered particles was analysed by employing experimental y vs. T curves for both alloys. Such experimental curves, shown in Fig. 2(a) and (b) (solid lines) were constructed from the thermograms reported by Matsuo and Clarenbrough [15] on continuous heating of slowly cooled samples. Gauding and Warlimont [16] performed electron microscopic measurements of particle radius in specimens cooled slowly from 773 K at a rate of 5.5 K h^{-1} to room temperature, giving values of 5 and 10 nm for the alloys containing 10 and 15 at.% Al, respectively. Also, activation energy values for self-diffusion are required as an input for the kinetic analysis. These values, computed by interpolation of recently reported data [17], are estimated to be 157 and 150 kJ mole^{-1} for 10 and 15 at.% of solute concentration, respectively.

Using the E and r_0 values already given for the alloy containing 15 at.% Al, a value of $K_{01} = 4.0 \times 10^{12}$ nm^2 s^{-1} was obtained after adjusting eqn. (9) to the experimental, y vs. T curve [Fig. 2(a), broken line]. It can be seen that the fit is rather poor. If this value of K_{01} is employed in order to fit the same kinetic law to the alloy containing 10 at.% Al by adjusting the domain radius, r_0 was found to be 5.3 nm. Although this predicted value of r_0 is in good agreement with that directly measured by TEM, the best fit shown in Fig. 2(b) (broken line) also does not follow the shape of the experimental y vs. T curve.

If on the other hand, eqn. (10) is fitted to the experimental y vs. T curve for the alloy containing 15 at.% Al [Fig. 2(a), dotted line], using the same values for E and r_0 already considered, $K_{02} = 7 \times 10^{12}$ nm^2 s^{-1}. A similar fit [Fig. 2(b), dotted line] resulted in a value of $r_0 = 5.1$ nm for the alloy containing 10 at.% Al after employing the same value of K_{02}. Conversely, by employing the appropriate values of E and r_0 for the Cu-10 at.% Al alloy, adjustment of the experimental y vs. T curve to eqn. (10) gave $K_{02} = 6 \times 10^{12}$ nm^2 s^{-1}. This in turn resulted in $r_0 = 10.2$ nm, after the same fit for the y vs. T experimental curve corresponding to the Cu-15 at. % Al alloy was made, by using the same value for K_{02}. This fit was as good as the latter one but it is not shown here for the sake of brevity.

It is then apparent that eqn. (10) can account for the domain size dependence on solute concentration and can also describe the dissolution kinetics of the ordered particles. Such a satisfactory description arises from the fact that the domains are spherical for the alloys under study [16,18],

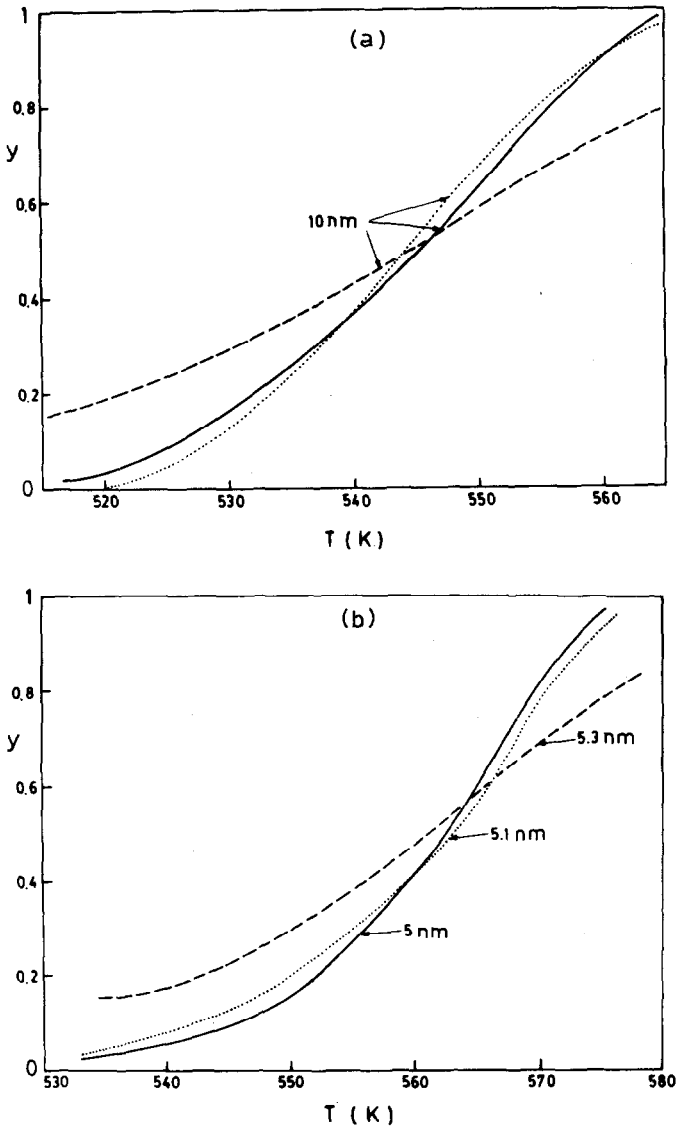

Fig. 2. (a) Experimental and calculated y vs. T curves for disperse order dissolution in Cu-15% at. Al. ———, Experimental curve; - - - - - -, calculated from eqn. (9); · · · · · ·, calculated from eqn. (10). Particle radius, 10 nm. (b) Experimental and calculated y vs. T curves for disperse order dissolution in Cu-10% at. Al. ———, Experimental curve; - - - - - -, calculated from eqn. (9); · · · · · ·, calculated from eqn. (10). Particle radius as indicated.

hence the kinetic law derived from the steady-state part of the diffusion field in spherical diffusion is a valid approximation for predicting the observed behaviour. It is worthwhile to notice that even for the case of thin disc-like precipitates, the diffusion field at large distances will be approximately spherical, and it is then expected that the results of eqn. (10) will apply at

long times for small volume fractions. The similar values obtained for K_{02} in both alloys indicates that the interdiffusion constant, D_0, is essentially insensitive to the solute concentration between 10 and 15 at.% Al.

The kinetic analysis performed here also enables us to predict particle size indirectly for a wider range of Al contents by employing an average value of K_{02} ($= 6.5 \times 10^{12}$ nm^2 s^{-1}), provided the experimental y vs. T curve is known in each case.

In closing, the fact that eqns. (9) and (10) are able to describe the kinetics of particle dissolution, each one for the specific shape of the precipitates considered here, verifies the hypothesis that K_1 and K_2 obey an Arrhenius equation and hence the kinetic models typified by eqns. (5) and (7) are suitable for use under non-isothermal conditions.

ACKNOWLEDGEMENTS

The authors wish to thank the Departamento de Desarrollo de la Investigación de la Universidad de Chile for financial support under Contract I.997.834.5 and to the Instituto de Investigaciones y Ensayes de Materiales, Facultad de Ciencias Físicas y Matemáticas, Universidad de Chile also for financial support and for the facilities given for this research.

REFERENCES

1 J. Burke, The Kinetics of Phase Transformations in Metals, Pergamon Press, Oxford, 1st edn., 1965, p. 40.
2 K. Asano and K. Hirano, Trans. Jpn. Inst. Met., 9 (1968) 24.
3 R.D. Iasi and P. Adler, Metall. Trans., 8A (1977) 1177.
4 H.B. Aaron, Met. Sci. J., 2 (1968) 192.
5 M.J. Whelan, Met. Sci. J., 3 (1969) 95.
6 R.A. Tanzilli and R.W. Heckel, Trans. TMS—AIME, 242 (1968) 2313.
7 R.A. Tanzilli and R.W. Heckel, Trans. TMS—AIME, 245 (1968) 1363.
8 H.S. Carslaw and J.C. Jaeger, Conduction of Heat in Solids, Clarendon Press, Oxford, 2nd edn., 1959, p. 247.
9 G. Thomas and M.J. Whelan, Philos. Mag., 6 (1961) 1103.
10 M.E. Brown and C.A.R. Phillipots, J. Chem. Educ., 55 (1978) 556.
11 W.D. Kingery, H.K. Bowen and D.R. Uhlman, Introduction to Ceramics, Wiley, New York, 2nd edn., 1976, pp. 421–422.
12 T. Ozawa, J. Therm. Anal., 9 (1976) 369.
13 J.M. Papazian, Metall. Trans., 13A (1982) 761.
14 J.B. Murphy, Acta Metall., 9 (1961) 563.
15 S. Matsuo and L.M. Clarenbrough, Acta Metall., 11 (1963) 1303.
16 W. Gauding and H. Warlimont, Z. Metallkd., 60 (1969) 488.
17 A. Varschavsky and E. Donoso, Metall. Trans., 14A (1983) 875.
18 A. Varschavsky, M.I. Pérez and T. Löbel, Metall. Trans., 6A (1975) 577.